J Mater Sci (2011) 46:5896–5902
DOI 10.1007/s10853-011-5675-5

Synthesis and electrochemical analyses of vapor-grown carbon fiber/pyrolytic carbon-coated $LiFePO_4$ composite

Fei Deng · Xierong Zeng · Jizhao Zou · Xiaohua Li

Received: 27 March 2011 / Accepted: 30 May 2011 / Published online: 9 June 2011

Abstract A vapor-grown carbon fiber/pyrolytic carbon-coated $LiFePO_4$ (VGCF/PCLFP) composite has been prepared in one step through a solid-state reaction accompanied by a gas-phase decomposition process. This method leads to the formation of a conductive network composed of pyrolytic carbon layer and in situ vapor-grown carbon fiber in the composite. The amount of carbon in the composite has been determined by a modified formula based on thermogravimetric analysis to be around 3.0 wt%. The optimized electrode of VGCF/PCLFP composite can deliver 150 $mAhg^{-1}$ at 0.5 C rate, 137 $mAhg^{-1}$ at 1.0 C rate and 132 $mAhg^{-1}$ at 3.0 C rate. And its discharge capacity loses only $\sim$4% at a higher rate of 3.0 C after 100 cycles. The area-specific impedance of a cell fabricated with VGCF/PCLFP composite is lower than that made of only pyrolytic carbon-coated $LiFePO_4$, reported here for the purpose of comparison. In comparison to the electrode made of carbon black/$LiFePO_4$ composite (10 wt% carbon), the charge transfer resistance of the VGCF/PCLFP composite electrode decreases from 165 to 91 Ω. This technique presents an attractive way to produce high-performance $LiFePO_4$ cathode material through a low-cost high-efficiency process.

F. Deng
School of Materials Science and Engineering, Northwestern Polytechnical University, 127 youyi xilu, Xi'an 710072, China
e-mail: fdeng80@yahoo.com.cn

X. Zeng (✉) · J. Zou · X. Li
College of Materials Science and Engineering, Shenzhen University, Nanhai Ave 3688, Shenzhen 518060, China
e-mail: zengxier@szu.edu.cn

X. Zeng · J. Zou · X. Li
Shenzhen Key Laboratory of Special Functional Materials, Nanhai Ave 3688, Shenzhen 518060, Guangdong, China

Introduction

The ever-growing demand for portable batteries with high energy density is exerting pressure for the development of advanced lithium-ion batteries. Conventional cathode materials for lithium-ion batteries such as layered $LiMO_2$ (M = Co, Ni, Mn) and the spinel $LiMn_2O_4$ have been the basis of most commercial cells [1, 2]. However, both of these materials have substantial limitations. Cobalt-oxide-based materials are costly, especially for large-scale applications such as backup power systems and hybrid electric vehicles, while cycling stability problems associated with $LiMn_2O_4$ have prohibited its commercial application [3]. In 1997, Padhi et al. [4] reported that $LiFePO_4$ (LFP) could be used as an ideal cathode material and showed it had a theoretical capacity of 170 $mAhg^{-1}$, little hygroscopicity and good thermal stability in its fully charged state. In addition, this material is inexpensive, nontoxic, and environmentally benign [5, 6]. However, the electronic conductivity of pure LFP (10^{-10} to 10^{-9} S cm^{-1} [7]) is by several orders of magnitude lower than that of other important cathode materials (10^{-3} S cm^{-1} for $LiCoO_2$ [8] or 10^{-4} S cm^{-1} for $LiMn_2O_4$ [9]), which limits its rate capability in lithium cells. Therefore, extensive studies have been conducted to overcome the weakness by using lattice doping [7] and/or surface coating methods [3, 10–12].

Pyrolytic carbon-coated LFP (PCLFP) composite was considered to be a novel and useful material by Belharouak et al. [11]. Their method could deposit pyrolytic carbon not only on the surface but also in the pores of the LFP particles. The as-prepared PCLFP composite could deliver 140 $mAhg^{-1}$ (25 °C) at 0.3 C rate without additional carbon black in the electrodes. Their technique could also reduce the amount of carbon (only 3.4 wt%) in the

electrodes, which is beneficial to improve the volumetric energy density and gravimetric energy density of the cell [13]. Recently, several other works using hydrocarbon gas as the carbon source have also been reported, where the gas–solid interface reaction yields carbon deposition on the particles [14–16]. Therefore, it is shown that the gas–solid reaction can produce a uniform carbon layer easily and result in a well-developed electronic conduction with a small amount of carbon.

Carbon materials have been reported as ideal conductive fillers in battery systems because of their high electrical and good corrosion resistance in many electrolytes [17–22]. Vapor-grown carbon fiber (VGCF), as a typical representative of advanced carbon materials, has been characterized in terms of the highly preferred orientation of their graphitic basal planes parallel to the fiber axis, with an annular ring texture in the cross section. This structure gives rise to excellent mechanical properties, very high electrical and thermal conductivity, and a high graphitizability of the fibers [23, 24]. Chen et al. reported that the first discharge capacity of VGCF-enhanced LFP composites was more than two times of those without VGCF [25]. Nevertheless, ball milling, the most widely used method to introduce carbon fibers in the mixing process [26–31], could inevitably increase the contact resistance and is difficult to ensure the homogenity and dipersity of the fibers in the eletrodes.

In this work, a vapor-grown carbon fiber/pyrolytic carbon-coated $LiFePO_4$ (VGCF/PCLFP) composite was prepared in one step through a solid-state reaction accompanied by a gas-phase decomposition process. This method presents a way to form an effective conductive network composed of pyrolytic carbon layer and in situ VGCF, which in turn leads to superior electrochemical performance.

Experimental

The precursor consisting of iron (II) oxalate, ammonium dihydrogen phosphate, and lithium carbonate in a stoichiometric molar ratio (1:1:1) was dispersed into acetone and then mixed by ball milling for 24 h. After evaporating the acetone, the mixture was decomposed at 320 °C for 12 h in argon, reground, and then heated to 700 °C at a rate of 10 °C min^{-1} in an oven under argon. Finally, the samples were sintered at 700 °C for 24 h. It was noted that a mixture of argon and propylene should be fed into the furnace chamber as soon as the temperature reaches 550 °C and then shut off when the mixture had been sintered at 700 °C for 2 h. For comparison, pure LFP was also obtained under the same conditions with the exception of gas-phase decomposition utilized in the synthesis process.

In order to determine the exact amount of carbon in the samples, thermogravimetric analysis (TGA, Q500, TA) was carried out under a dry air flow. The samples were heated to 700 °C at a rate of 5 °C min^{-1}.

X-ray diffraction (XRD, D8 ADVANCE, Bruker AXS) with Cu K_α radiation was used to identify the phases. An integrated Raman spectroscopy system (inVia Reflex, Renishaw) was used to analyze the structure and composition. The excitation wavelength was supplied by an internal Ar (514.5 nm) 20 mW laser. Field emission scanning electron microscopy (FESEM, S-4800, HITACHI) and energy dispersive X-ray spectroscopy (EDS, EDAX) were used to analyze the morphology and elementary components, respectively. High resolution transmission electron microscopy (HRTEM, JEM-2100F) was used to analyze the nanostructure of the samples.

For comparison, two kinds of electrodes were made in this study, one which contains 92 wt% active material (VGCF/PCLFP composite) and 8 wt% polyvinylidene fluoride (PVDF), and the other which consists of 82 wt% active material (pure LFP), 10 wt% carbon black and 8 wt% PVDF. Both electrodes were prepared by spreading a slurry in *N*-methylpyrrolidone onto aluminum foil current collectors and allowing them to dry. 2032-size coin cells were assembled in an argon-filled glove box (UNILab2000, M. Braun) using lithium as a counter electrode and 1 M $LiPF_6$ in 1:2 ethylene carbonate/dimethyl carbonate (EC-DMC) as the electrolyte solution. Charge/discharge tests were performed using an Arbin Instruments (BT2000) at 25 °C.

The area-specific impedance (ASI) measurements were performed using a 30 s current interruption method every 30 min during the charge/discharge cycling.

The electrochemical impedance spectroscopy (EIS) was measured with a frequency response analyzer (Solatron 1260) interfaced with a potentio-galvanostat (Solatron 1287). The sinusoidal excitation voltage applied to the cells was 10 mV rms with a frequency range of between 10^4 and 10^{-1} Hz. We analyzed the impedance data to evaluate the equivalent circuit parameters by using a parameter fitting program (Scribner Associates, Zplot for Windows).

Results and discussion

Figure 1a shows the XRD plot of the VGCF/PCLFP composite. All intense peaks in the pattern can be attributed to orthorhombic LFP (JCPDS Card No. 83-2092, space group Pnma (62), $a = 10.334$ Å, $b = 6.01$ Å, $c = 4.693$ Å) while the absence of peaks corresponding to graphite indicated that the carbon in the sample was not well crystallized. The Raman spectrum of the as-prepared composite is shown in Fig. 1b. The bands at 500–100 cm^{-1} and

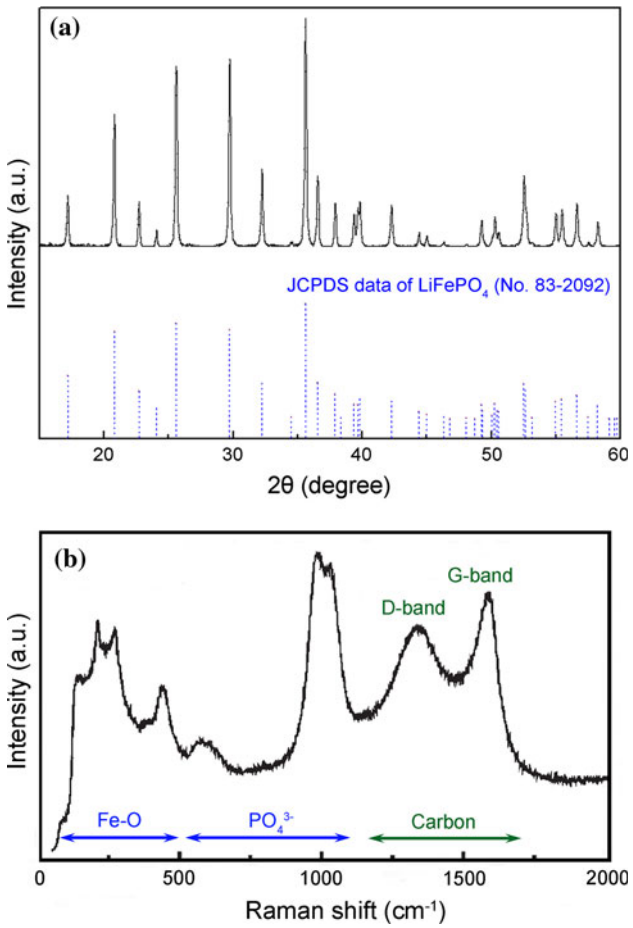

Fig. 1 **a** XRD plot and **b** Raman spectrum of VGCF/PCLFP composite

1,120–520 cm^{-1} correspond to the Raman vibrations of Fe–O and PO_4^{3-} in LFP, respectively, while the bands in the range of 1,460–1,170 cm^{-1} and 1,730–1,470 cm^{-1} can be assigned to the disorder-induced phonon mode (D-band) and the graphite band (G-band) of carbon, respectively [32, 33]. These results reveal that the as-prepared sample was mainly composed of LFP and amorphous carbon.

Figure 2a shows an FESEM photograph of the VGCF/PCLFP composite. The average size of irregularly shaped particles was around 500 nm and they were mainly composed of Fe, P, O, and C element (Fig. 2d). Combined with the XRD and Raman analyses above, these particles are likely to be pyrolytic carbon-coated LFP. In addition, many needle-like fibers formed at the surface of those particles, some of which were oriented arrangement parallel or perpendicular to the surface of the particles (indicated by arrows in Fig. 2a). More interesting is their in situ growth mode which can be seen in the further magnified image shown in Fig. 2b. The HRTEM image indicates that the in situ fibers exhibited typical VGCF microstructure which was reported in detail by Endo et al. [18, 19]. The as-prepared VGCF had an average diameter of about 25 nm, which is indicative of their excellent electrical conductivity and mechanical strength [19]. The selected area diffraction patterns (SADP) of the composite are given in Fig. 2e and f. The vapor-deposited pyrolytic carbon layer homogeneously covering the surface of LFP particles had a uniform thickness of less than 2.5 nm and formed an effective conductive network together with VGCF in the composite. Both the pyrolytic carbon layer and VGCF resulted from the decomposition of propylene, and the formation of VGCF may have been assisted by the catalytic action of iron and/or iron compounds during the process [18, 19]. However, there was no evidence that they existed in the as-prepared composite, which may echo previous studies regarding the preparation of VGCF without any catalysts [34, 35], though further research is still needed.

The products after the TGA experiment performed on the VGCF/PCLFP composite can be indexed to $Li_3Fe_2(PO_4)_3$ and Fe_2O_3 (Fig. 3a), which is consistent with the report of Belharouak et al. [11]. As a result, the weight change with respect to the oxidation of the VGCF/PCLFP composite in the TGA curve may take place according to the Eq. 1:

$$nC - LiFePO_4 + \frac{1}{4}O_2 \uparrow + nO_2 \uparrow \longrightarrow \frac{1}{3}Li_3Fe_2(PO_4)_3 + \frac{1}{6}Fe_2O_3 + nCO_2 \uparrow \quad (1)$$

As a consequence, the amount of carbon in the VGCF/PCLFP composite is calculated to be around 3.0 wt% according to the Eq. 2:

$$\%\text{carbon} = (M_{LFP} - M_{C-LFP}) * \delta \quad (2)$$

where M_{LFP} and $M_{C\text{-}LFP}$ are the weight gain of pure LFP and VGCF/PCLFP composite after TGA experiments performed at a temperature range of 25–700 °C, and the variable, δ, is defined according to the Eq. 3:

$$\delta = \frac{1}{1 + M_{LFP}} \quad (3)$$

Here M_{LFP} and $M_{C\text{-}LFP}$ are equal to 5.03 and 1.9 wt% (from Fig. 3b), respectively. This formula is more accurate than that proposed by Belharouak et al. [11] because of the consideration of variable (δ).

Figure 4 shows the initial charge/discharge curves of VGCF/PCLFP composite at different rates. In the potential range of 2.5–4.2 V, the composite delivered 155 $mAhg^{-1}$ with 95% cycle efficiency at 0.2 C rate in the first cycle, and it delivered 150 $mAhg^{-1}$ at 0.5 C rate, 137 $mAhg^{-1}$ at 1.0 C rate, and 132 $mAhg^{-1}$ at 3.0 C rate. For comparison, Chen and Dahna reported that the discharge capacity of C/LFP was 110 $mAhg^{-1}$ at 2 C rate when the carbon content was 7% [13], and Belharouak et al. reported that

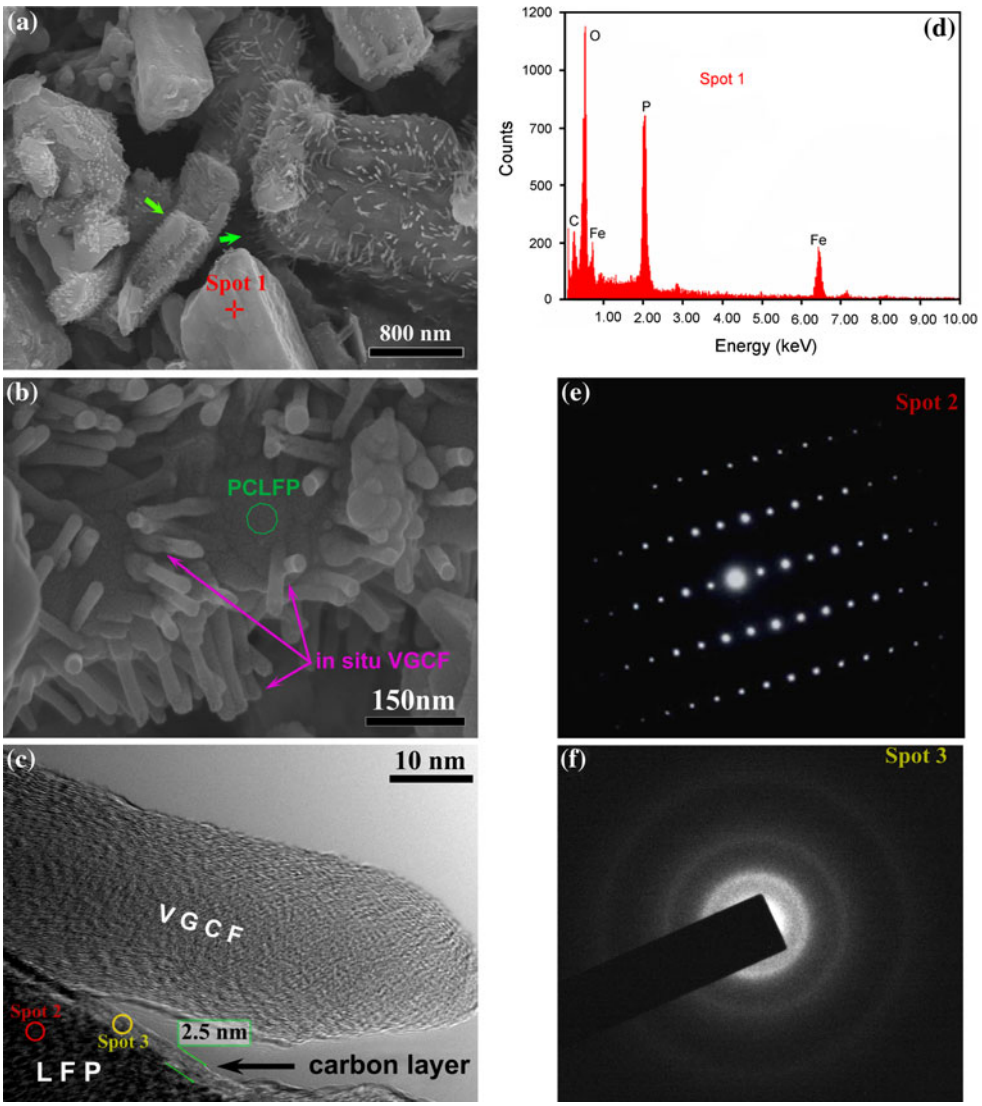

Fig. 2 **a** FESEM photograph of VGCF/PCLFP composite, **b** higher magnification FESEM image of VGCF/PCLFP composite, **c** HRTEM image of VGCF/PCLFP composite, **d** EDS analysis of spot 1, **e** selected area diffraction pattern (SADP) of spot 2, and **f** SADP of spot 3

PCLFP released 140 $mAhg^{-1}$ at 0.3 C rate when the carbon content was 3.4 wt% [11]. Thus, the electrochemical property of the cathode material obtained by our technique is notably improved. It is known that lithium ion intercalation/deintercalation reactions depend on electronic conduction [36]. In this study, the conductive network composed of pyrolytic carbon layer and VGCF enabled active material to transport lithium ions and electrons in mass at a fast rate. Furthermore, the diffusion of lithium ions, which is considered to be the slowest process, depending on the porosity of the electrode to a certain extent, can also be improved by the formation of VGCF.

The cycling performance of the VGCF/PCLFP composite is given in Fig. 5. The capacity fading on cycling VGCF/PCLFP composite at 0.2 C rate was negligible after 100 cycles, and the capacity lost only ~4% at 3.0 C rate after 100 cycles.

Figure 6 shows the ASI curves of PCLFP reported by Belharouak et al. [11] and VGCF/PCLFP composite produced by our process. For the cells made of VGCF/PCLFP composite with ~3.0 wt% carbon, the ASI is obviously lower than that of PCLFP composite electrode. This implies that the combination of pyrolytic carbon layer and VGCFs can improve the conductivity of the electrode effectively. It is worthy of special mention that the excellent properties of VGCF may play an even greater role despite its little quantity [19].

Figure 7 compares the electrochemical impedance spectra of the VGCF/PCLFP composite electrode (3.0 wt% carbon) and the carbon black/LFP composite electrode (10 wt% carbon). The interpretation of the impedance spectra is based on the equivalent circuit shown in Fig. 7. Where R_s represents the sum of the ohmic resistance of the research system, CPE (constant phase element) represents

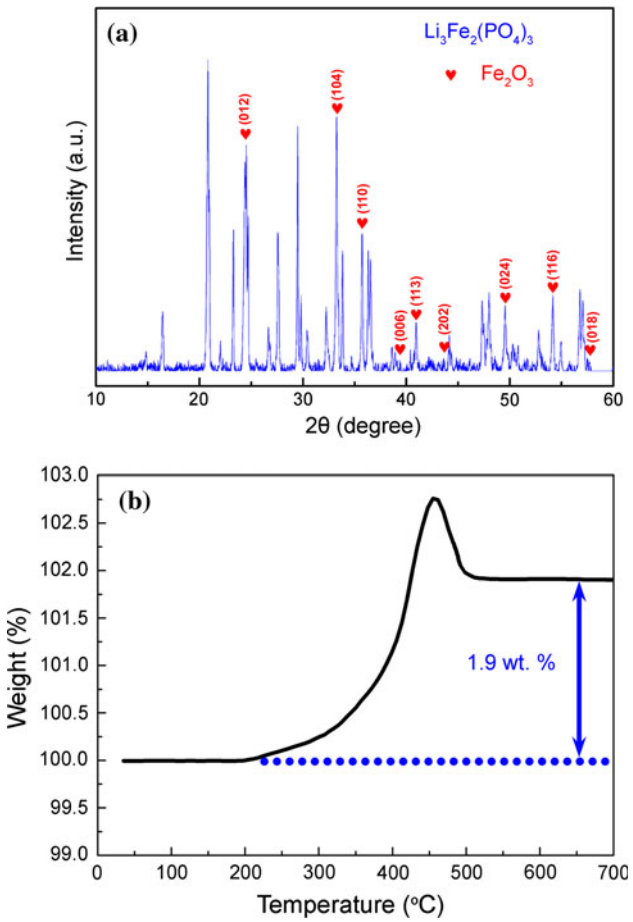

Fig. 3 **a** XRD plot of the resulting products after TGA of VGCF/PCLFP composite performed under dry air and **b** TGA curve of VGCF/PCLFP composite

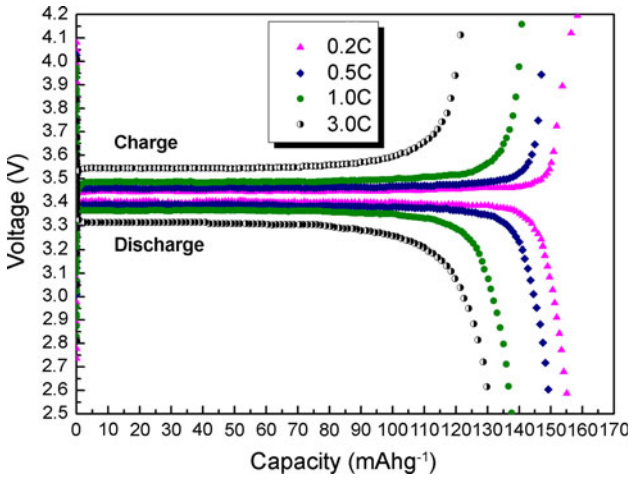

Fig. 4 Charge/discharge curves of VGCF/PCLFP composite electrode at the cutoff voltage of 2.5–4.2 V versus Li/Li^+ at different rate in 1 M $LiPF_6$/EC-DMC (1:2) at 25 °C

the double layer capacitance, and the SEI (solid electrolyte interface) film capacitance instead of a capacitor to compensate for nonhomogeneity in the system, R_{ct} is a charge

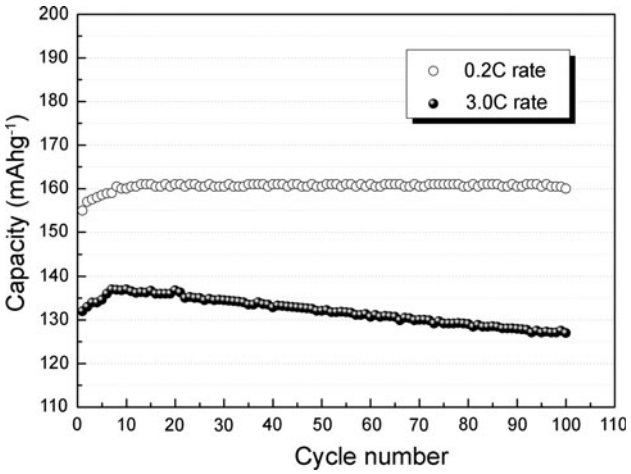

Fig. 5 Plots of discharge capacities of VGCF/PCLFP composite electrode as a function of the cycle number in the first 100 cycles at the cutoff voltage of 2.5–4.2 V versus Li/Li^+ at different rate in 1 M $LiPF_6$/EC-DMC (1:2) at 25 °C

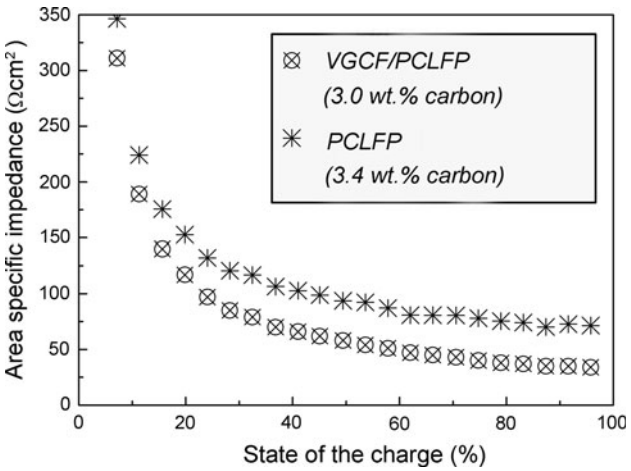

Fig. 6 ASI curves of the different LFP cathode materials

transfer resistor which is related to the electrochemical reaction at the electrode–electrolyte interface and particle–particle contact and Z_w is the finite length Warburg with a short circuit terminus [37–39]. Some of the parameters obtained by fitting are listed in Table 1. In the high-frequency region, the charge transfer resistance of the VGCF/PCLFP composite electrode and the carbon black/LFP composite electrode is 91 and 165 Ω, respectively. This change could be attributed to the replacement of carbon black by the conductive network wired by pyrolytic carbon layer and VGCF. In the low-frequency region, the impedance slope of VGCF/PCLFP composite electrode is bigger than that of carbon black/LFP composite electrode, indicating that vapor-deposited pyrolytic carbon layer and VGCF were able to enhance the electrochemical activity of LFP more effectively than carbon black.

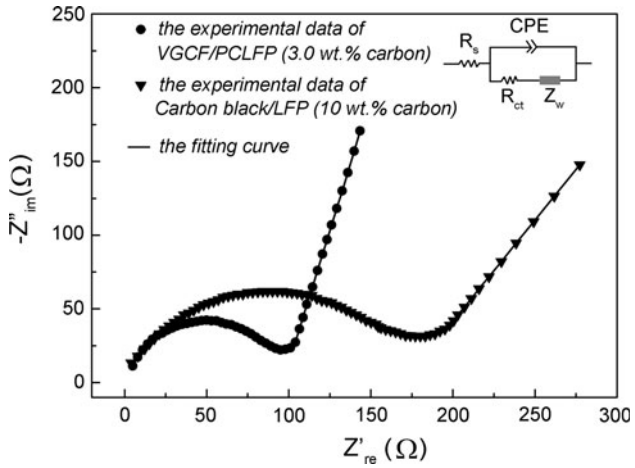

Fig. 7 EIS spectra of carbon black/LFP composite electrode and VGCF/PCLFP composite electrode in 1 M $LiPF_6$/EC-DMC (1:2) at 25 °C in the frequency range from 0.1 to 10 kHz

Table 1 EIS fitting results of VGCF/PCLFP and carbon black/LFP

Parameter	VGCF/PCLFP (3.0 wt% carbon)	Carbon black/LFP (10 wt% carbon)
R_s/Ω	8.386	9.671
R_{ct}/Ω	91.2	165.3
Z_w-R/Ω	74.35	158.34
CPE–T/μF	18.73	8.521
CPE–n	0.93	0.82

Conclusions

A VGCF/PCLFP composite has been prepared in one step through a solid-state reaction accompanied by a gas-phase decomposition process. The olivine structure ($LiFePO_4$, Pnma (62)) was not affected using our technique. The amount of carbon in the composite was determined to be around 3.0 wt% using a modified formula based on TGA. The electrode fabricated with VGCF/PCLFP composite delivered a discharge capacity of 150 $mAhg^{-1}$ at 0.5 C rate, 137 $mAhg^{-1}$ at 1.0 C rate and 132 $mAhg^{-1}$ at 3.0 C rate. The ASI of the cell fabricated with VGCF/PCLFP composite was lower than that made of single pyrolytic carbon-coated $LiFePO_4$. Additionally, compared to the electrode made of carbon black/$LiFePO_4$ composite (10 wt% carbon), the charge transfer resistance of the VGCF/PCLFP composite electrode decreased from 165 to 91 Ω. The improvement of electrochemical properties was mainly attributed to the formation of an effective conductive network composed of vapor-deposited pyrolytic carbon layer and in situ VGCF. This study provides a feasible way to achieve high-performance $LiFePO_4$ cathode material through a simple low-cost high-efficiency process.

Acknowledgements This work was supported by the Two Hundred Plan for Talent Station of Shenzhen (Shenfu [2008] No.182), the Science and Technology R&D Program of Shenzhen (CXB201005240010A), the Science and Technology R&D Program of Shenzhen (ZD200904290044A), the Science and Technology Project of Shenzhen (JC200903130266A), and the fund of Shenzhen Key Laboratory of Special Functional Materials (T201005). We also thank Professor Wenjun Liu for his technical guidance with electrochemical impedance spectroscopy.

References

1. Whittingham MS (2004) Chem Rev 104:4271
2. Li H, Wang ZX, Chen LQ, Huang XJ (2009) Adv Mater 21:4593
3. Huang H, Yin SC, Nazarz LF (2001) Electrochem Solid State Lett 4:A170
4. Padhi AK, Najundaswamy KS, Goodenough JB (1997) J Electrochem Soc 144:1188
5. Padhi AK, Nanjundaswamy KS, Masquelier C, Okada S, Goodenough JB (1997) J Electrochem Soc 144:1609
6. Padhi AK, Nanjundaswamy KS, Masquelier C, Goodenough JB (1997) J Electrochem Soc 144:2581
7. Chung SY, Bloking JT, Chiang YM (2002) Nat Mater 1:123
8. Molenda J, Stoklosa A, Bak T (1989) Solid State Ionics 36:53
9. Guan J, Liu M (1998) Solid State Ionics 110:21
10. Ravet N, Goodenough JB, Besner S, Simoneau M, Hovington P, Armand M (1999) In: 196th meeting of the electrochemical society, Honolulu, HI, p 127
11. Belharouak I, Johnson C, Amine K (2005) Electrochem Commun 7:983
12. Croce F, Epifanio AD, Hassoun J, Deptula A, Olczac T, Scrosatia B (2002) Electrochem Solid State Lett 5:A47
13. Chen ZH, Dahna JR (2002) J Electrochem Soc 149:A1184
14. Zhao B, Jiang Y, Zhang HJ, Tao HH, Zhong MY, Jiao Z (2009) J Power Sources 189:462
15. Marcinek ML, Wilcox JW, Doeff MM, Kosteckia RM (2009) J Electrochem Soc 156:A48
16. Nakamura T, Shima Y, Matsui H, Yamada Y, Hashimoto S, Miyauchi H, Koshiba N (2010) J Electrochem Soc 157:A544
17. Tatsumi K, Zaghib K, Sawada Y, Abe H, Ohsaki T (1995) J Electrochem Soc 142:1090
18. Endo M, Nishimura Y, Takahashis T, Takeuchi K, Dresselhaus MS (1996) J Phys Chem Solids 57:725
19. Endo M, Kim YA, Hayashi T, Nishimurab K, Matusitaa T, Miyashitaa K, Dresselhaus MS (2001) Carbon 39:1287
20. Utsunomiya H, Nakajima T, Ohzawa Y, Mazej Z, Zemvab B, Endo M (2010) J Power Sources 195:6805
21. Fraczek-Szczypta A, Bogun M, Blazewicz S (2009) J Mater Sci 44:4721. doi:10.1007/s10853-009-3730-2
22. Kercher AK, Kiggans JO, Dudney NJ (2010) J Electrochem Soc 157:A1323
23. Speck JS, Endo M, Dresselhaus MS (1989) J Cryst Growth 94:834
24. Tibbetts GG (1983) Appl Phys Lett 42:666
25. Chen CC, Liu MH, Chen JM (2004) In: 206th meeting of the electrochemical society, Honolulu, HI, p 413
26. Lin Q, Harb JN (2004) J Electrochem Soc 151:A1115
27. Sheem K, Lee YH, Lim HS (2006) J Power Sources 158:1425
28. Li XL, Kang FY, Shen WC (2006) Carbon 44:1334
29. Li XL, Kang FY, Bai XD, Shen WC (2007) Electrochem Commun 9:663
30. Sotowa C, Origi G, Takeuchi M, Nishimura Y, Takeuchi K, Jang IY, Kim YJ, Hayashi T, Kim YA, Endo M, Dresselhaus MS (2008) ChemSusChem 1:911

31. Jin B, Jin EM, Park KH, Gu HB (2008) Electrochem Commun 10:1537
32. Burba CM, Frech R (2004) J Electrochem Soc 151:A1032
33. Wu XL, Jiang LY, Cao FF, Guo YG, Wan LJ (2009) Adv Mater 21:2710
34. Zou JZ, Zeng XR, Xiong XB, Tang HL, Li L, Liu Q (2007) Carbon 45:828
35. Ajayan PM, Nugent JM, Siegel RW, Wei B, Kohler-Redlich P (2000) Nature 404:243
36. Dominko R, Gaberscek M, Drofenik J, Bele M, Pejovnik S, Jamnik J (2003) J Power Sources 119–121:770
37. Zhou YK, He BL, Zhou WJ, Li HL (2004) J Electrochem Soc 151:A1052
38. Lee CY, Tsai HM, Chuang HJ, Li SY, Lin P, Tseng TY (2005) J Electrochem Soc 152:A716
39. Choia YM, Pyun SI (1997) Solid State Ionics 99:173